J. of Supercritical Fluids 85 (2014) 183–189

Contents lists available at ScienceDirect

The Journal of Supercritical Fluids

journal homepage: www.elsevier.com/locate/supflu

Improvement mechanism of resistance random access memory with supercritical CO_2 fluid treatment

Kuan-Chang Chang[a], Jung-Hui Chen[b], Tsung-Ming Tsai[a], Ting-Chang Chang[c,i,*], Syuan-Yong Huang[a], Rui Zhang[d], Kai-Huang Chen[e], Yong-En Syu[c], Geng-Wei Chang[f], Tian-Jian Chu[a], Guan-Ru Liu[c], Yu-Ting Su[c], Min-Chen Chen[c], Jhih-Hong Pan[a], Kuo-Hsiao Liao[a], Ya-Hsiang Tai[f], Tai-Fa Young[g], Simon M. Sze[c,h], Chi-Fong Ai[j], Min-Chuan Wang[j], Jen-Wei Huang[k]

[a] Department of Materials and Optoelectronic Science, National Sun Yat-Sen University, 70 Lien-hai Road, Kaohsiung 804, Taiwan
[b] Department of Chemistry, National Kaohsiung Normal University, Kaohsiung, Taiwan
[c] Department of Physics, National Sun Yat-Sen University, 70 Lien-hai Road, Kaohsiung 804, Taiwan
[d] School of Software and Microelectronics, Peking University, Beijing 100871, People's Republic of China
[e] Department of Electronics Engineering and Computer Science, Tung-Fang Design Institute, Kaohsiung, Taiwan
[f] Department of Photonics and the Institute of Electro-Optical Engineering, National Chiao Tung University, Hsinchu 300, Taiwan
[g] Department of Mechanical and Electro-Mechanical Engineering, Kaohsiung 804, Taiwan
[h] Department of Electronics Engineering and Institute of Electronics, National Chiao Tung University, Hsinchu 300, Taiwan
[i] Advanced Optoelectronics Technology Center, National Cheng Kung University, Taiwan
[j] Physics Division, Institute of Nuclear Energy Research, Taoyuan, Taiwan
[k] Department of Physics, ROC Military Academy, Kaohsiung 83055, Taiwan

ARTICLE INFO

Article history:
Received 22 August 2012
Received in revised form 30 August 2013
Accepted 4 September 2013

Keywords:
Supercritical fluid
RRAM
Hydration–dehydration reaction
Tin doping

ABSTRACT

We demonstrated that the supercritical CO_2 fluid treatment was a new concept to efficiently reduce the operation current of resistance random access memory. The dangling bonds of tin-doped silicon oxide ($Sn:SiO_x$) thin film were passivated by the hydration–dehydration reaction through supercritical CO_2 fluid treatment, which was verified by the XPS and FTIR analyses. The current conduction mechanism of low resistance state in post-treated $Sn:SiO_x$ thin film was transferred to hopping conduction from Ohmic conduction. Furthermore, the current conduction mechanism of high resistance state in the memory device was transferred to Schottky emission from Frenkel–Poole conduction. The phenomena were attributed to the discontinuous metal filament formed by hydration–dehydration reaction in $Sn:SiO_x$ thin film through supercritical fluid treatment. Finally, a reaction model was proposed to explain the mechanism of current reduction in $Sn:SiO_x$ thin film with supercritical CO_2 fluid treatment.

1. Introduction

For the increasing demands for portable electronic products, nonvolatile memory has been widely applied as information storage device due to its low power consumption properties. Modern semiconductor nonvolatile memories are scaled constantly to achieve large capacity while device features approach the sub-100-nm regime. However, the increasing demand for device densities by scaling dimension is expected to be a major challenge due to the technical and physical limitation. To surmount the technical and physical limitation issues of conventional charge storage-based memories [1–8], the resistance random access memory (RRAM) constructed of an insulating layer sandwiched by two electrodes is widely investigated by industries and academics. The RRAM is a great potential candidate for next-generation nonvolatile memory due to their superior characteristics such as lesser cost, simple structure, high-speed operation, and non-destructive readout [9,10]. Various materials have been reported to possess resistive switching behaviors, such as solid-electrolyte-based RRAM [11,12], transition metal oxides (MnO_x, ZrO_x, HfO_x) [13–15,9,16,17], and organic material [18]. In addition, many switching mechanism of RRAM have been proposed to explain resistive switching phenomenon, such as conductive filaments [19], valence change [20], and Schottky barrier [21]. However, the underlying mechanism of resistive switching behavior is still not yet understood clearly. Silicon-based oxide is a promising material for RRAM applications because of its great compatibility in integrated circuit (IC) process.

* Corresponding author at: Department of Physics, National Sun Yat-Sen University, 70 Lien-hai Road, Kaohsiung 804, Taiwan. Tel.: +866 7 5252000x3708; fax: +886 7.
E-mail address: tcchang@mail.phys.nsysu.edu.tw (T.-C. Chang).

0896-8446/$ – see front matter.
http://dx.doi.org/10.1016/j.supflu.2013.09.002

Therefore, the research using silicon-based oxide as the resistance-switching layer was worthy of investigation.

In our preceding research, supercritical CO_2 ($SCCO_2$) fluid technology was used to improve the dielectric properties and performance of various thin film transistors (TFTs), such as hydrogenated amorphous-silicon TFTs and ZnO TFTs [22–30]. Supercritical phase is peculiar with its characteristics of high penetration of gas and solubility of liquid. The supercritical water fluid has tremendous oxidation property [31]. However, high critical temperature and high critical pressure are essential condition to achieve supercritical water fluid, which is difficult to realize through modern facilities. By adding a little water into supercritical CO_2 fluids, the liquid water can attain to the supercritical fluid phase due to the phase close to idea solution.

In this work, tin metal doped into silicon oxide by co-sputtering at room temperature was taken as the resistance switching layer of RRAM. To evaluate the resistive switching properties of tin-doped silicon oxide (Sn:SiO_x) layer, the Pt/Sn:SiO_x/TiN device was fabricated at clean room. Moreover, the material and conduction mechanism analyses were executed to explain the influence of Sn metal doped in silicon oxide on resistive switching behaviors. In addition, the Pt/$SCCO_2$-treated Sn:SiO_x/TiN sandwiched devices were fabricated to investigate the effect of $SCCO_2$ on resistive switching properties of Sn:SiO_x thin film. The effects of $SCCO_2$ treatment on resistive switching behaviors of Sn:SiO_x thin film was also evaluated by material and carrier conduction mechanism analyses. Furthermore, the reaction mechanism in RRAM with $SCCO_2$ fluid was also discussed to explain the reason of electrical property improvement on Sn:SiO_x RRAM.

2. Experimental

The experimental specimens were prepared as follows: In the first group, the Sn:SiO_x thin film (about 30 nm) was deposited on the TiN/Ti/SiO_2/Si substrate by co-sputtering with the pure SiO_2 and Sn targets. The sputtering power was fixed at RF power 200 W and 3 W for SiO_2 and Sn targets respectively. The co-sputtering was executed in argon ambient (Ar = 30 sccm) with a working pressure of 0.789 Pa at room temperature. In the second group, the Sn:SiO_x thin films were put into the reactive chamber of supercritical fluid system, and then the $SCCO_2$ fluid mixed with 0.5 ml water were syringed into the reactive chamber to treat the specimens. The passivation efficiency increases with the rising of temperature and CO_2 pressure as long as exceeding the critical point, which are 31 °C with 7.3 MPa CO_2. But owing to the limitation of our experiment equipment, the water-mixed supercritical CO_2 fluids were heated and pressured to 120 °C and 20.4 MPa in the stainless steel chamber of supercritical fluid system for 1 h. Finally, the Pt top electrode of 200 nm thickness was deposited on Sn:SiO_x thin film to form electrical devices with Pt/Sn:SiO_x/TiN sandwich structures by DC magnetron sputtering. By contrast, the Pt/SiO_2/TiN sandwich structures were made by same process procedure with a sputtered SiO_2 layer instead of a Sn:SiO_x layer as control samples. The entire electrical measurements of devices with the Pt electrode of 250 μm diameter were performed using Agilent B1500 semiconductor parameter analyzer. Besides, the Fourier transform infrared spectroscopy (FTIR) measured by Bruker VERTEX 70v spectrometer in far infrared region and X-ray photoelectron spectroscopy (XPS) were used to analyze the chemical composition and bonding of these insulator materials, respectively.

3. Results and discussion

The "forming process" is required to activate all of the Sn:SiO_x RRAM devices, using dc voltage sweeping with a compliance current of 2 mA. The leakage current of the Sn:SiO_x RRAM devices after $SCCO_2$ treatment was lower than that of pre-treatment devices (Fig. 1). This phenomenon is attributed to the improvement on dielectric properties through $SCCO_2$ treatment, which has been reported by our previous study [23]. The voltage sweep bias was applied on TiN electrode with the grounded Pt electrode as shown in the bottom left inset of Fig. 2. After the forming process, a gradual decrease in current was observed where the cell switches from low resistance state (LRS) to high resistance state (HRS), called as "reset process", by sweeping the voltage from 0 to −1.8 V without current compliance. On contrast, as the voltage was swept from 0 to 1.2 V with a 5 mA current compliance, the resistance switched from HRS to LRS, called as "set process". In the Pt/Sn:SiO_x/TiN device, the resistance ratio of HRS and LRS is about 10^2 times at a reading voltage of 0.1 V. The electrical current-voltage properties of the Sn:SiO_x devices were compared before and after $SCCO_2$ treatment (Fig. 2). The current of Sn:SiO_x devices is reduced at 0.1 V reading voltage after $SCCO_2$ treatment. To investigate the interesting phenomena, we analyzed the current conduction mechanism of Sn:SiO_x thin film with and without $SCCO_2$ treatment as shown in Fig. 3. The carrier transport in LRS state of Sn:SiO_x device was dominated by Ohmic conduction in the Sn:SiO_x layer. After $SCCO_2$ treatment, the current conduction mechanism will transfer to hopping conduction because of the change of material properties. In addition, we also analyzed the current conduction mechanism in HRS of Sn:SiO_x with and without $SCCO_2$ treatment as shown in Fig. 4. The relationship in the curve of ln(I/V) versus the square root

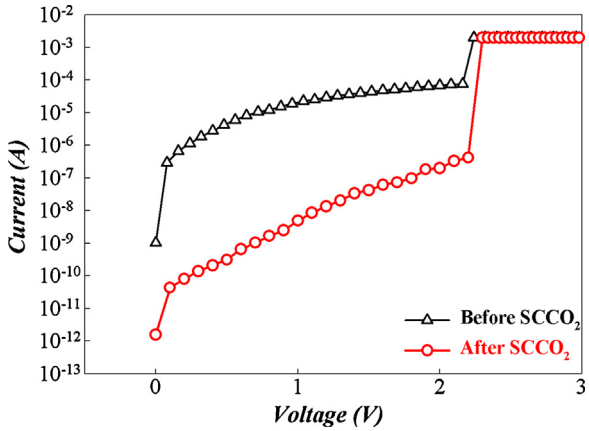

Fig. 1. The forming current curves of the Sn:SiO_x RRAM devices before and after $SCCO_2$ treatment.

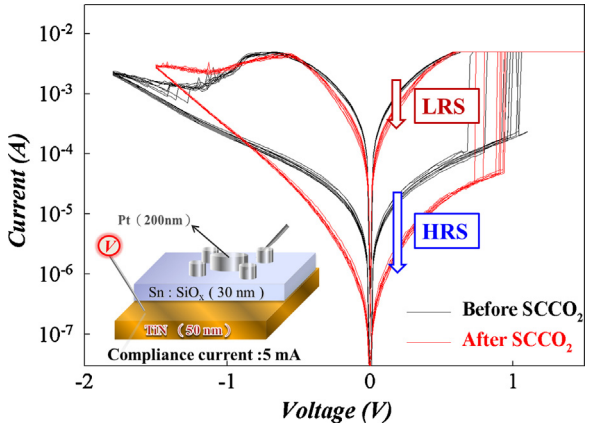

Fig. 2. The black and red curves are the resistive switching characteristics of Sn:SiO_x film before and after $SCCO_2$ treatment, respectively. The current in high resistance state of post-treated Sn:SiO_x film is reduced about 15 times from 9 μA to 0.6 μA.

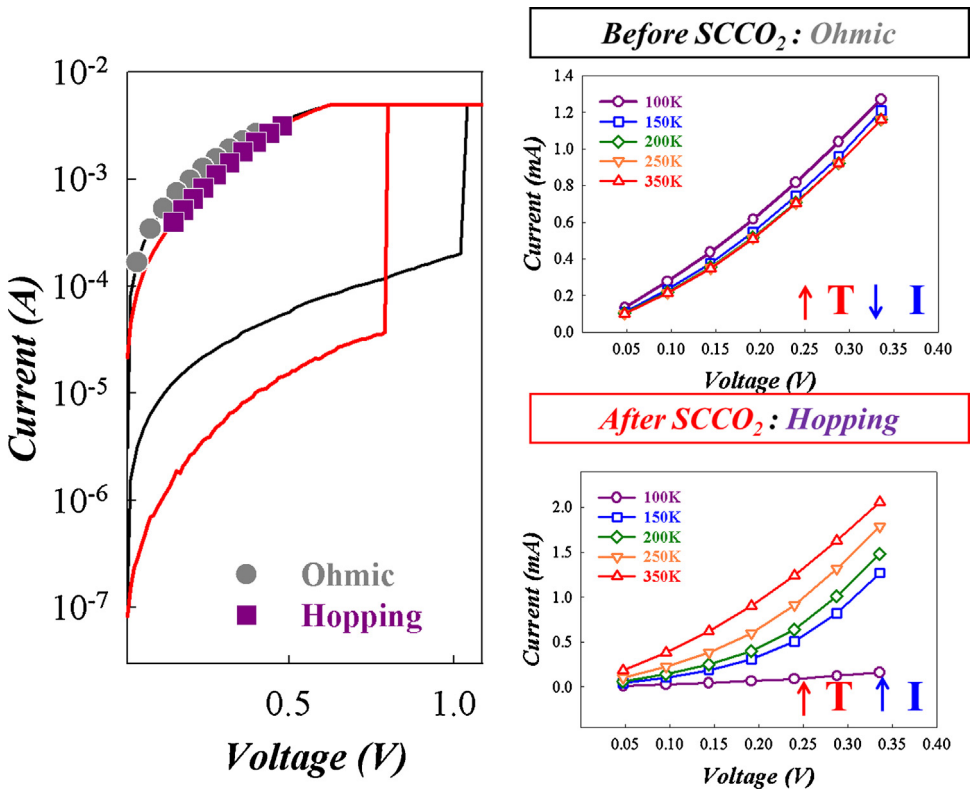

Fig. 3. The current conduction curves in the LRS of Sn:SiO_x devices before and after $SCCO_2$ treatment. The current vs. voltage diagrams were measured at different temperature environments in the Sn:SiO_x film before and after $SCCO_2$ treatment.

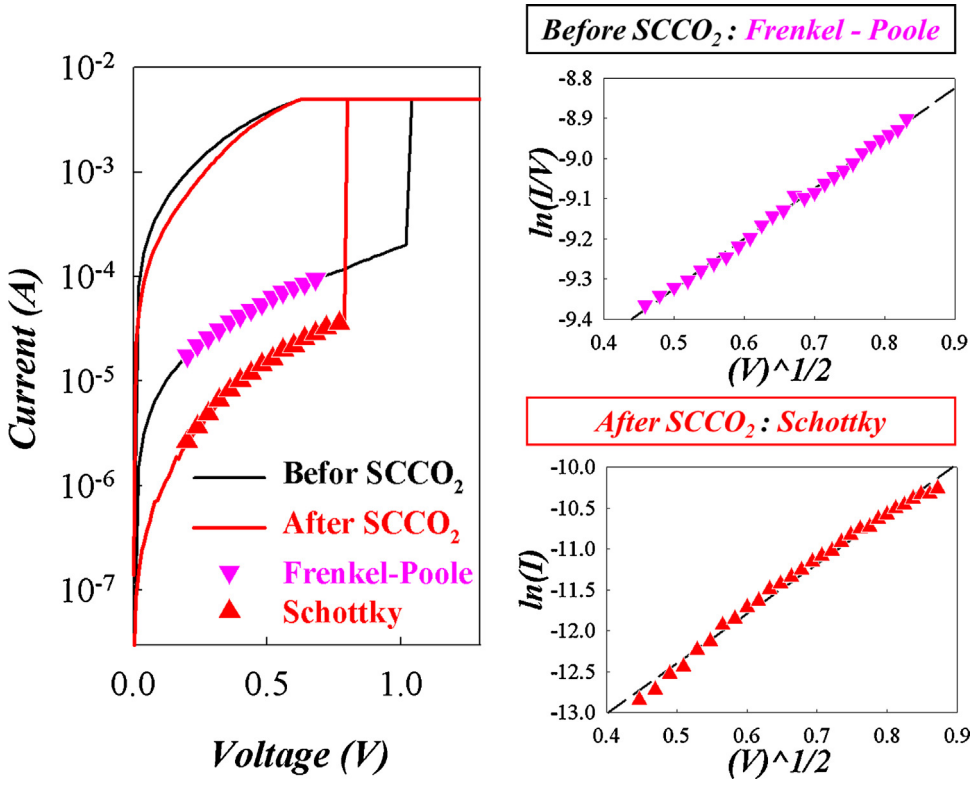

Fig. 4. The current conduction curves in the HRS of Sn:SiO_x devices before and after $SCCO_2$ treatment. The fitting of current vs. voltage curves in the HRS of the devices before and after $SCCO_2$ treatment was drawn in right side.

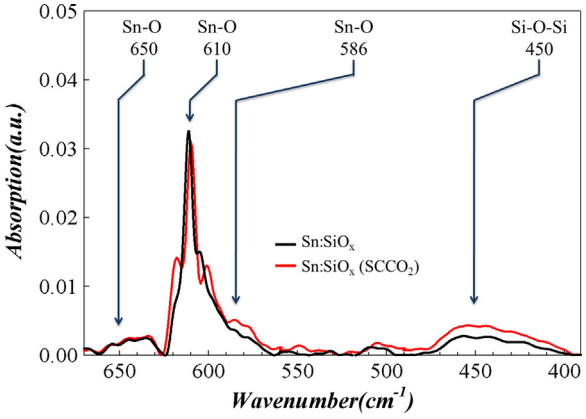

Fig. 5. The comparison of FTIR spectra of Sn:SiO_x film before and after $SCCO_2$ treatment. Both intensity of Sn—O and Si—O—Si bonds are increased in Sn:SiO_x film after $SCCO_2$ treatment.

of the applied voltage ($V^{1/2}$) is linear. According to the relationship of Frenkel–Poole conduction, $I \propto V \exp[(q/kT)(2a\sqrt{V} - \phi_{Bt})]$, where a is $\sqrt{q/4\pi\varepsilon_i d}$, ϕ_{Bt} is the trap barrier height, and d is the insulator thickness. The Frenkel–Poole conduction is due to emission of trapped electrons into conduction band. The supply of electrons from the traps is through thermal excitation. The barrier reduction is larger than in the case of Schottky emission by a factor of 2, which can be obtained as compared with the slope of the plot of ln(I) versus ($V^{1/2}$) based on the formula of Schottky emission, $I \propto I^2 \exp[(q/kT)(a\sqrt{V} - \phi_B)]$, where ϕ_B is the Schottky barrier height. The results revealed that the carrier transport of Sn:SiO_x film was dominated by Frenkel–Poole conduction due to the trap in the film. After $SCCO_2$ treatment, the current conduction mechanism will transfer to Schottky emission because of the improvement of dielectric properties. Therefore, we utilized the material spectra analyses to find out the reason of different electrical transfer mechanisms in conduction current before and after $SCCO_2$ treatment. Compared the FTIR spectra of Sn:SiO_x film with and without $SCCO_2$ treatment (Fig. 5), we found that the absorption peak of Sn-O bond at 586 cm^{-1} was increased after $SCCO_2$ treatment. The result implies that the density of Sn—O bond was increased in the Sn:SiO_x film after $SCCO_2$ treatment. In addition, the absorption of Si—O—Si stretch bond at 450 cm^{-1} was also increased after $SCCO_2$ treatment, illustrating the content of silicon oxide bonding in the film also increased [32,33]. To analyze the chemical composition of Sn:SiO_x film in this study, X-ray photoelectron spectroscopy (XPS) of Sn $3d_{5/2}$, Si 2p and O 1s peaks were performed. After compared with the peak area of Sn, Si and O XPS spectra, the mole fraction of Sn: Si: O in the co-sputtered Sn:SiO_x film was 0.3%: 29.5%: 70.2%. According to XPS spectra analyses for Sn $3d_{5/2}$ core level (Fig. 6), the mole fraction of Sn—O bond was obviously risen but that of Sn element was decreased in Sn:SiO_x film after $SCCO_2$ treatment. Besides, the mole fraction of Si—O bond was substantially increased in contrast with that of Si—OH bond after $SCCO_2$ treatment in terms of the XPS spectra analyses of Si 2p core level as shown in Fig. 6. Table 1 shows the comparison of the areas of deconvolution peaks of Sn $3d_{5/2}$ and Si 2p core levels. We found the mole fraction (SnO_2:Sn = 50.6%:49.4%) in Sn:SiO_x film is changed to that (SnO_2:Sn = 70.6%:29.4%) after $SCCO_2$ treatment. Also, the mole fraction (SiOH:SiO_2 = 18.9%:81.1%) in Sn:SiO_x film is changed to that (SiOH:SiO_2 = 66.4%:33.6%) in the post-treated Sn:SiO_x film. Therefore, we infer that the level of oxidation would increase and

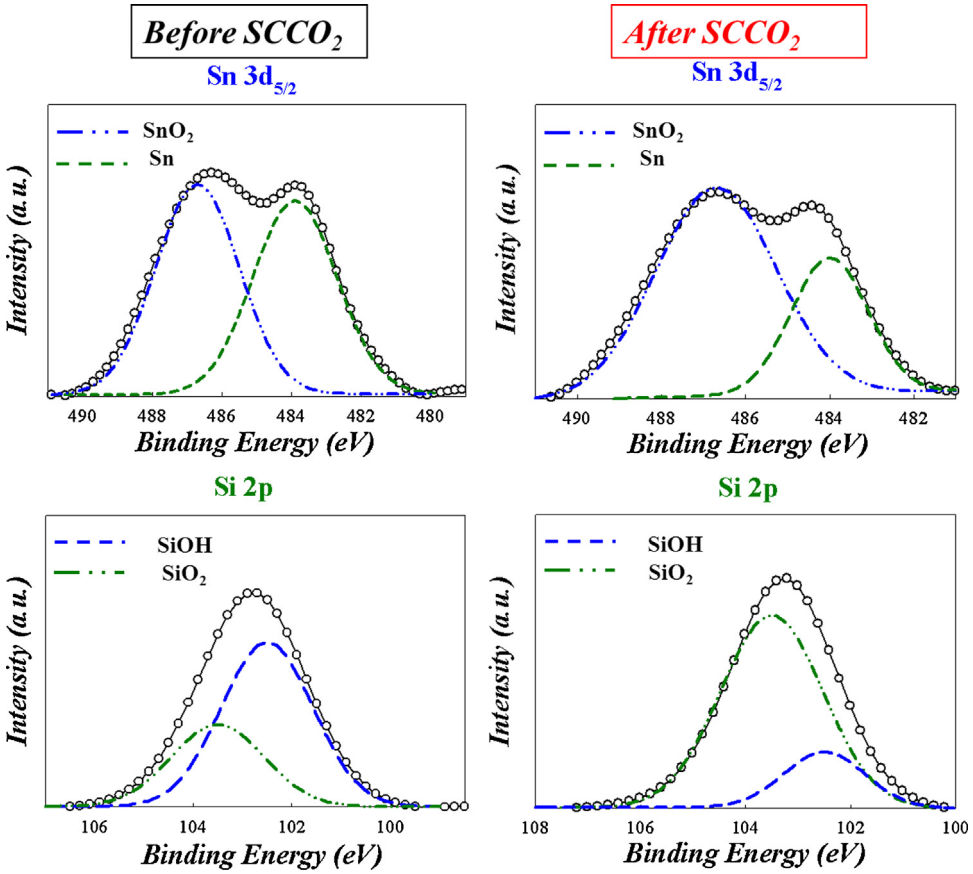

Fig. 6. XPS spectra of Sn $3d_{5/2}$ and Si 2p core levels in Sn:SiO_x film before and after $SCCO_2$ treatment. The mole fraction of metallic tin and Si—OH bonds in Sn:SiO_x film are reduced obviously but that of tin oxide and silicon oxide bonds are increased after $SCCO_2$ treatment.

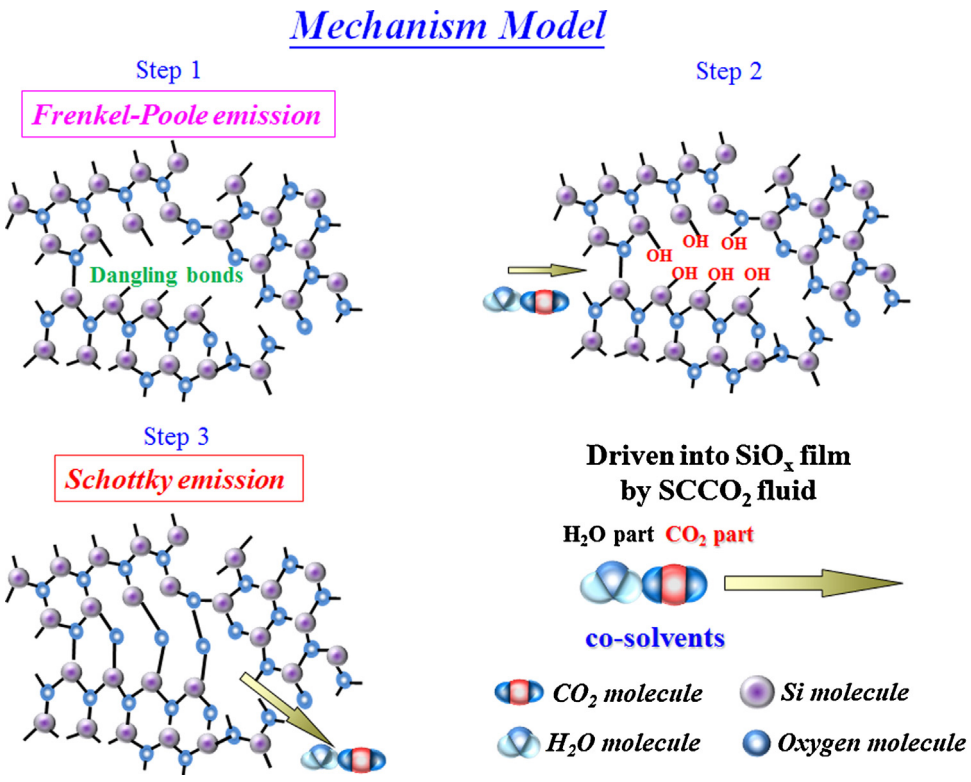

Fig. 7. The schematic diagram of hydration–dehydration reaction mechanism on Sn:SiO_x film to illustrate defect passivation through $SCCO_2$ treatment.

Table 1
Comparison of the areas of deconvolution peaks of Sn $3d_{5/2}$ and Si 2p core levels before and after $SCCO_2$ treatment.

	SnO_2	Sn	SiOH	SiO_2
Before $SCCO_2$	50.6%	49.4%	66.4%	33.6%
After $SCCO_2$	70.6%↑	29.4%↓	18.9%↓	81.1%↑

accompany with dehydration in the post-treated film. These results were consistent with the above-mentioned FTIR analyses.

Based on the electrical and material analyses, we proposed a reaction mode to explain reaction mechanism of Sn:SiO_x film with $SCCO_2$ treatment as shown in Fig. 7. As the sample was put into the water-mixed $SCCO_2$ fluid environment, the H_2O molecule was carried into the grain boundary of Sn:SiO_x film by $SCCO_2$ fluid, which is attributed to the high penetration ability of $SCCO_2$ fluid. As the H_2O molecule approached to grain boundary of the film, the hydration reaction occurred in the Sn:SiO_x film. Then, monomolecular CO_2 in supercritical fluids induces the dehydration of neighbor hydroxyl groups so as to form Si—O—Si and Sn—O—Si network-like bonding in the film. The mechanism is call hydration–dehydration reaction of $SCCO_2$ fluids in Sn:SiO_x film. As for the LRS of Sn:SiO_x film, the conductive filament will be formed in pre-treated Sn:SiO_x film after the forming process. The conductive filament will be connected with dangling bond in the switching region of the film. The carriers were transported through these dangling bonds, leading to the current conduction dominated by Ohmic conduction. If the Sn:SiO_x film was put into the $SCCO_2$ fluid environment, the H_2O molecule was carried into the grain boundary of the film by $SCCO_2$ fluid, which is attributed to the high penetration ability of $SCCO_2$ fluid. Hence, the tin metal in Sn:SiO_x thin film will be isolated due to hydration–dehydration reaction by $SCCO_2$ treatment. Only if the conductive filament formed in the Sn:SiO_x film, the carrier will hop through the isolated tin metal in the switching region of the post-treated film. This phenomena will make the electrical current conduction in LRS of Sn:SiO_x film transferred from Ohmic conduction to hopping conduction as shown in Fig. 8. Owing to the trap of Sn:SiO_x film can be passivated by $SCCO_2$ treatment, the electrical current conduction in HRS of Sn:SiO_x film will be transferred to Schottky emission from Frenkel–Poole conduction as shown in Fig. 9. This phenomenon will cause the improvement of dielectric properties of thin film, leading to decrease the operation current and the power consumption of RRAM.

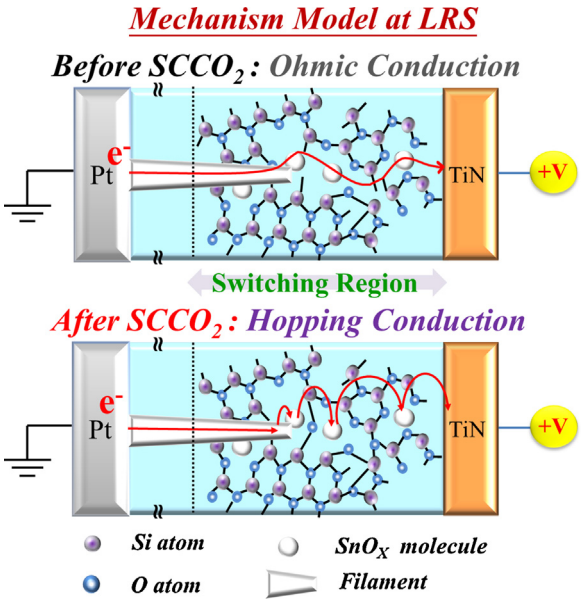

Fig. 8. The schematic diagram of carrier hopping model in Sn:SiO_x film after $SCCO_2$ treatment.

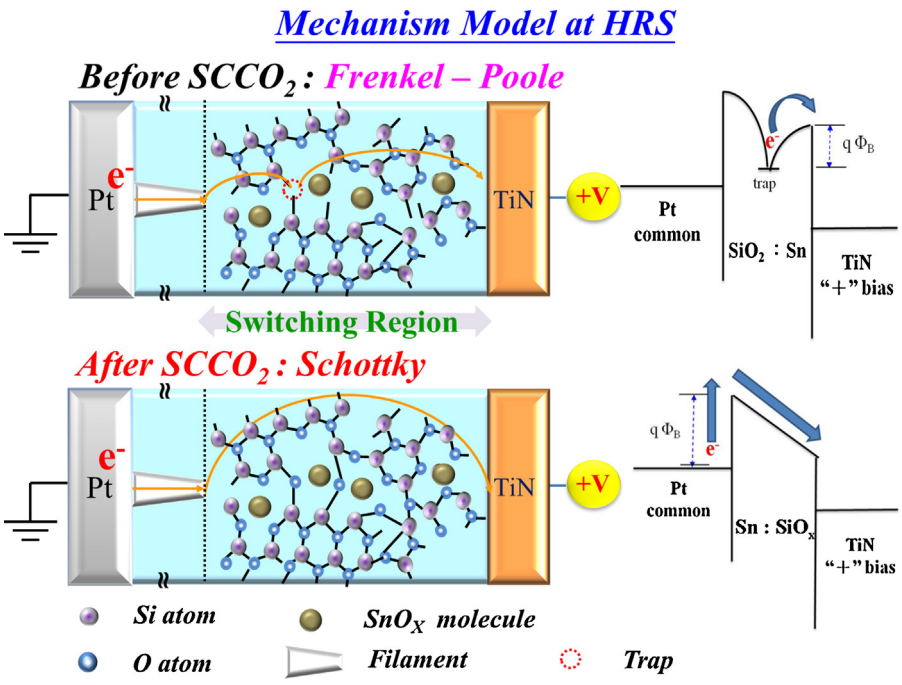

Fig. 9. The schematic diagram of the transfer on carrier conduction mechanism in Sn:SiO_x film after $SCCO_2$ treatment.

4. Conclusion

In summary, the operation current of Sn-doped silicon oxide RRAM device was reduced by supercritical fluid treatment in this study. The water molecular can be brought into the film to passivate the dangling bond of grain boundary in resistive switching layer by supercritical CO_2 fluid. In virtue of the phenomena, the discontinuous conductive filament in Sn:SiO_x film was formed by hydration–dehydration reaction through $SCCO_2$ fluids. The operation current of RRAM can be reduced due to the decrease of defect in the layer, which results in low power consumption. Besides, the effect of joule heating can also be improved for the device. Therefore, supercritical fluid treatment can enhance the properties of resistive switching layer of RRAM device. We believe that the technology is beneficial to the development of RRAM for the next generation nonvolatile applications.

Acknowledgments

This work was performed at the National Science Council Core Facilities Laboratory for Nano-Science and Nano-Technology in the Kaohsiung-Pingtung area and was supported by the National Science Council of the Republic of China under Contract Nos. NSC-102-2120-M-110-001, and NSC 101-2221-E-110-044-MY3.

References

[1] T.C. Chang, F.Y. Jian, S.C. Chen, Y.T. Tsai, Developments in nanocrystal memory, Materials Today 14 (12) (2011) 608–615.
[2] D. Jiang, M. Zhang, Z. Huo, Q. Wang, J. Liu, Z. Yu, X. Yang, Y. Wang, B. Zhang, J. Chen, M. Liu, A study of cycling induced degradation mechanisms in Si nanocrystal memory devices, Nanotechnology 22 (2011) 254009.
[3] F.M. Yang, T.C. Chang, P.T. Liu, P.H. Yeh, Y.C. Yu, J.Y. Lin, S.M. Sze, J.C. Lou, Memory characteristics of Co nanocrystal memory device with HfO_2 as blocking oxide, Applied Physics Letters 90 (2007) 132102.
[4] J. Liu, Q. Wang, S. Long, M. Zhang, M. Liu, Metal/Al_2O_3/ZrO_2/SiO_2/Si (MAZOS) structure for high-performance non-volatile memory application, Semiconductor Science and Technology 25 (2010) 055013.
[5] C.H. Liu, Y. Kuo, Nanocrystalline ruthenium oxide embedded zirconium-doped hafnium oxide high-k nonvolatile memories, J. Applied Physics 110 (2011) 024101.
[6] C. Zhu, Z. Huo, Z. Xu, M. Zhang, Q. Wang, J. Liu, S. Long, M. Liu, Performance enhancement of multi-level cell nonvolatile memory by using a bandgap engineered high-k trapping layer, Applied Physics Letters 97 (2010) 253503.
[7] F.M. Yang, T.C. Chang, P.T. Liu, U.S. Chen, P.H. Yeh, Y.C. Yu, J.Y. Lin, S.M. Sze, J.C. Lou, Nickel nanocrystals with HfO_2 blocking oxide for nonvolatile memory application, Applied Physics Letters 90 (2007) 222104.
[8] C. Zhu, Z. Xu, Z. Huo, R. Yang, Z. Zheng, Y. Cui, J. Liu, Y. Wang, D. Shi, G. Zhang, F. Li, M. Liu, Investigation on interface related charge trap and loss characteristics of high-k based trapping structures by electrostatic force microscopy, Applied Physics Letters 99 (2011) 223504.
[9] S. Zhang, S. Long, W. Guan, Q. Liu, Q. Wang, M. Liu, Resistive switching characteristics of MnO_x-based ReRAM, J. Physics D: Applied Physics 42 (2009) 055112.
[10] Y.E. Syu, T.C. Chang, T.M. Tsai, Y.C. Hung, K.C. Chang, M.J. Tsai, M.J. Kao, S.M. Sze, Redox reaction switching mechanism in RRAM device with Pt/CoSiOX/TiN structure, IEEE Electron Device Letters 32 (2011) 545–547.
[11] Q. Liu, S. Long, H. Lv, W. Wang, J. Niu, Z. Huo, J. Chen, M. Liu, Controllable growth of nanoscale conductive filaments in solid-electrolyte-based ReRAM by using metal nanocrystal cover bottom electrode, ACS Nano 4 (10) (2010) 6162–6168.
[12] Q. Liu, J. Sun, H. Lv, S. Long, K. Yin, N. Wan, Y. Li, L. Sun, M. Liu, Real-time observation on dynamic growth/dissolution of conductive filaments in oxide-electrolyte-based ReRAM, Advanced Materials 24 (14) (2012) 1844–1849.
[13] Q. Liu, C. Dou, Y. Wang, S. Long, W. Wang, M. Liu, M. Zhang, J. Chen, Formation of multiple conductive filaments in the Cu/ZrO_2:Cu/Pt device, Applied Physics Letters 95 (2009) 023501.
[14] Q. Liu, S. Long, W. Wang, Q. Zuo, S. Zhang, J. Chen, M. Liu, Improvement of resistive switching properties in ZrO_2-based ReRAM with implanted Ti ions, IEEE Electron Device Letters 30 (12) (2009) 1335–1337.
[15] M. Liu, Z. Abid, W. Wang, X. He, Q. Liu, W. Guan, Multilevel resistive switching with ionic and metallic filaments, Applied Physics Letters 94 (2009) 233106.
[16] Y. Wang, Q. Liu, S. Long, W. Wang, Q. Wang, M. Zhang, S. Zhang, Y. Li, Q. Zuo, J. Yang, M. Liu, Investigation of resistive switching in Cu-doped HfO_2 thin film for multilevel non-volatile memory applications, Nanotechnology 21 (2010) 045202.
[17] Y. Li, S. Long, M. Zhang, Q. Liu, S. Zhang, Y. Wang, Q. Zuo, S. Liu, M. Liu, Resistive switching properties of Au/ZrO_2/Ag structure for low voltage nonvolatile memory applications, IEEE Electron Device Letters 31 (2) (2010) 117–119.
[18] X. Liu, Z. Ji, D. Tu, L. Shang, J. Liu, M. Liu, C. Xie, Organic nonpolar nonvolatile resistive switching in poly(3,4-ethylene-dioxythiophene): polystyrenesulfonate thin film, Organic Electronics 10 (6) (2009) 1191–1194.
[19] J.Y. Son, Y.H. Shin, Direct observation of conducting filaments on resistive switching of NiO thin films, Applied Physics Letters 92 (2008) 222106.
[20] A. Beck, J.G. Bednorz, C. Gerber, C. Rossel, D. Widmer, Reproducible switching effect in thin oxide films for memory applications, Applied Physics Letters 77 (2000) 139–141.
[21] T. Fujii, M. Kawasaki, A. Sawa, H. Akoh, Y. Kawazoe, Y. Tokura, Hysteretic current–voltage characteristics and resistance switching at an epitaxial oxide Schottky junction $SrRuO_3$/$SrTi_{0.99}Nb_{0.01}O_3$, Applied Physics Letters 86 (2005) 012107.
[22] C.T. Tsai, T.C. Chang, P.T. Liu, P.Y. Yang, Y.C. Kuo, K.T. Kin, P.L. Chang, F.S. Huang, Low-temperature method for enhancing sputter-deposited HfO_2 films with complete oxidization, Applied Physics Letters 91 (2007) 012109.

[23] C.T. Tsai, T.C. Chang, K.T. Kin, P.T. Liu, P.Y. Yang, C.F. Weng, F.S. Huang, A low temperature fabrication of HfO_2 films with supercritical CO_2 fluid treatment, J. Applied Physics 103 (7) (2008) 074108.
[24] M.C. Chen, T.C. Chang, S.Y. Huang, K.C. Chang, H.W. Li, S.C. Chen, J. Lu, Y. Shi, A low-temperature method for improving the performance of sputter-deposited ZnO thin-film-transistors with supercritical fluid, Applied Physics Letters 94 (2009) 162111.
[25] C.T. Tsai, P.T. Liu, T.C. Chang, C.W. Wang, P.Y. Yang, F.S. Yeh, Low-temperature passivation of amorphous-silicon thin-film transistors with supercritical fluids, IEEE Electron Device Letters 28 (2007) 584–586.
[26] C.T. Tsai, T.C. Chang, P.T. Liu, Y.L. Cheng, K.T. Kin, F.S. Huang, Application of supercritical CO_2 fluid for dielectric improvement of SiO_x film, Electrochemical and Solid-State Letters 12 (2009) H35–H37.
[27] M.C. Chen, T.C. Chang, S.Y. Huang, K.C. Chang, H.C. Huang, S.C. Chen, J. Liu, D.S. Gan, N.J. Ho, T.F. Young, G.W. Jhang, Y.H. Tai, Improvement of the performance of ZnO TFTs by low-temperature supercritical fluid technology treatment, Surface & Coatings Technology 204 (2009) 1112–1115.
[28] K.C. Chang, T.M. Tsai, T.C. Chang, Y.E. Syu, H.C. Hung, Y.C. Hung, T.F. Young, D.S. Gan, N.J. Ho, Low-temperature synthesis of ZnO nanotubes by supercritical CO_2 fluid treatment, Electrochemical and Solid-State Letters 14 (2011) K47–K50.
[29] K.C. Chang, T.M. Tsai, T.C. Chang, Y.E. Syu, C.C. Wang, S.L. Chuang, C.H. Li, D.S. Gan, S.M. Sze, Reducing operation current of Ni-doped silicon oxide resistance random access memory by supercritical CO_2 fluid treatment, Applied Physics Letters 99 (2011) 263501.
[30] K.C. Chang, T.M. Tsai, T.C. Chang, Y.E. Syu, S.L. Chuang, C.H. Li, D.S. Gan, S.M. Sze, The effect of silicon oxide based RRAM with tin doping, Electrochemical and Solid-State Letters 15 (2012) H65–H68.
[31] Y. Kikuchi, K. Kurata, J. Nakatani, M. Hirao, Y. Oshima, Analysis of supercritical water oxidation for detoxification of waste organic solvent in university based on life cycle assessment, J. Hazardous Materials 194 (2011) 283–289.
[32] R.K. Singh, A. Srinivasan, Bioactivity of ferrimagnetic MgO-CaO-SiO_2-P_2O_5-Fe_2O_3 glass-ceramics, Ceramics International 36 (2010) 283–290.
[33] R. Rai, T.D. Senguttuvan, S.T. Lakshmikumar, Study of the electronic and optical bonding properties of doped SnO_2, Computation Materials Science 37 (2006) 15–19.